

MINIATURIZATION OF p-GE LASERS

PROGRESS TOWARD A TUNABLE, CONTINUOUS WAVE THz LASER

E. Bründermann (Email: Erik.Bruendermann@DLR.de), A.M. Linhart and H.P. Röser

DLR, Institute for Space Sensor Technology, Rudower Chaussee 5, D-12489 Berlin, Germany

O.D. Dubon, W.L. Hansen and E.E. Haller

Lawrence Berkeley National Laboratory and University of California, Berkeley, CA 94720, USA

Abstract

We have observed laser action in Al-doped germanium crystals with volumes as small as 0.025 cm^3 , one order of magnitude smaller than previously studied p-Ge laser crystals. The duty cycle was improved by two orders of magnitude up to 2×10^{-3} . Improved crystal and heat sink design, high quality ohmic contacts and external resonators may offer an opportunity to build a powerful, tunable and continuous wave THz laser.

1. Introduction

We are developing a compact, tunable and continuous wave (CW) THz laser. Such a laser would be valuable as a local oscillator in heterodyne receivers for studying far-infrared rotational transitions of molecules in starforming regions [1], in atmospheric research [2] and in solid state spectroscopy [3]. The detection of faint astronomical signals in the THz-range is only possible above the troposphere from airplanes and satellites due to the strong water absorption lines at sea level. The limited space, power and time of flight require compactness, continuous wave operation and low power consumption. One of the most promising devices with reasonable output power in the THz frequency range is the pulsed p-type Ge laser in crossed electric and magnetic fields operated at liquid helium temperature (LHe) [4, 5].

2. p-Ge laser mechanism

Laser action in these devices is based on an inversion of the hole population between the light and heavy hole bands for magnetic fields in the range of 0.25 to 2.5 T. For higher magnetic fields up to 4.5 T the light hole bands are separated significantly into Landau levels. In the high B-field regime cyclotron resonance (CR) lasing transitions within the light hole band occur by emitting single line laser radiation which is tunable by the magnetic field. The intervalence band (IVB) transitions produce broad band multiline laser emission which can be controlled and tuned by an external resonator.

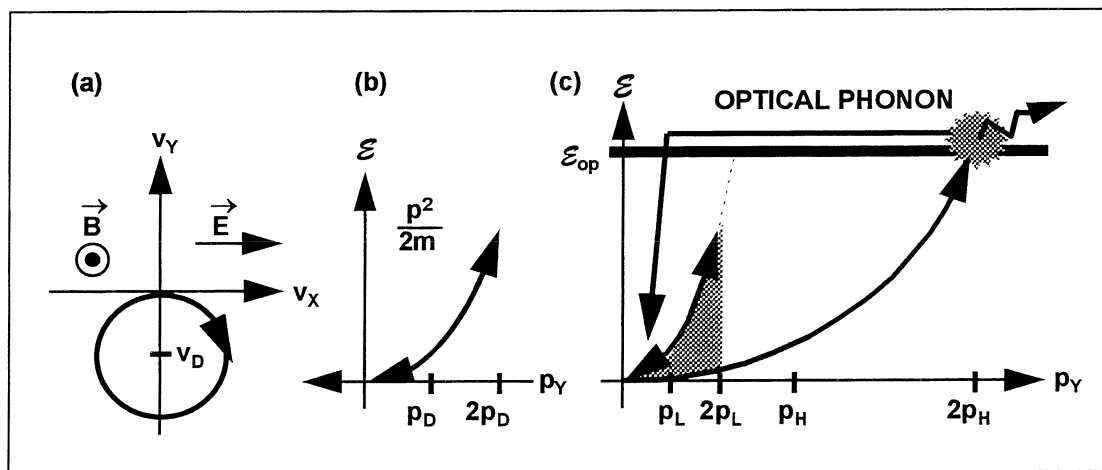


Figure 1. (a) The main trajectory of holes at 4.2 K in crossed electric E and magnetic B fields can be approximated as an orbit in velocity space through the origin surrounding the drift center $v_D = E/B$. (b) In the energy-momentum diagram the oscillation from (a) translates into an oscillation on the band ($p_D = mE/B$ with m the hole effective mass). (c) For the light hole mass m_L and the heavy hole mass m_H different maximum energies are reached ($p_L = m_L E/B$, $p_H = m_H E/B$). For the light holes we obtain $E_{L,MAX} = (2p_L)^2/(2m_L)$ and for the heavy holes $E_{H,MAX} = (2p_H)^2/(2m_H)$, respectively. While $E_{H,MAX}$ is above and $E_{L,MAX}$ below the optical phonon energy of 37 meV the upper band is populated due to heavy hole optical phonon scattering into the light hole band leading to laser emission distributed over a wide energy range (gray area).

To obtain IVB lasing it is necessary to induce an inversion between the hole populations in the light and heavy hole bands. The first requirement is a lattice temperature below 20 K which is achieved by immersing it into liquid helium at 4.2 K (figure 1(a)). At these temperatures acoustical lattice scattering is negligible and optical lattice scattering is not possible. Excitation by a high electric field between 0.33 and 3.5 kV/cm accelerates holes above the optical phonon energy leading to strong backscattering into

the valence band. The electric field of 0.33 kV/cm defines the onset of heavy hole streaming motion. If at the same time a magnetic field is applied, the light holes can be 'trapped' into an orbit where the maximum energy is always less than the optical phonon energy of 37 meV, while at the same time the heavy holes exceed this energy and scatter with a 4% chance into the light hole band (figure 1(c)). Thus, a situation is created where the lifetime of the light holes (upper laser level) is much longer than that of heavy holes (lower laser level) and inversion is produced

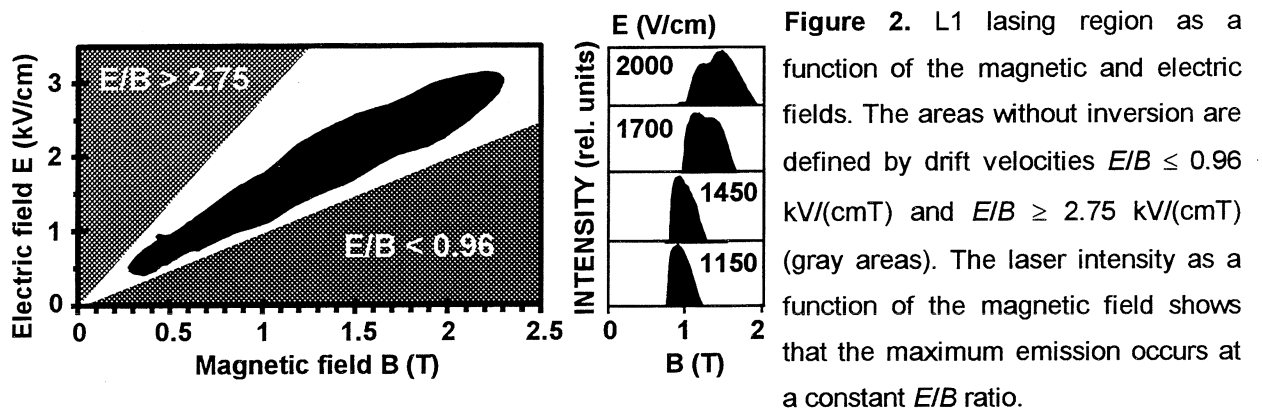


Figure 2. L1 lasing region as a function of the magnetic and electric fields. The areas without inversion are defined by drift velocities $E/B \leq 0.96$ kV/(cmT) and $E/B \geq 2.75$ kV/(cmT) (gray areas). The laser intensity as a function of the magnetic field shows that the maximum emission occurs at a constant E/B ratio.

For a drift velocity of $E/B \leq 0.96$ kV/(cmT) = 0.96×10^5 m/s the maximum heavy and light hole energies are below 37 meV and the inversion cannot be established while the pumping mechanism of optical phonon scattering is not populating the light hole level. The maximum light hole energy for $E/B \geq 2.75$ kV/(cmT) is above 37 meV therefore the light holes rapidly emit optical phonons decreasing the lifetime in the upper laser level. Figure 2 displays the lasing region of L1 (Table 1) and shows the areas without inversion. The broad band gain allows multimode laser emission over the range 1 to 4.5 THz [4].

3. Spectral purity

Figure 3 shows the laser emission of a p-Ge laser crystal as a result of selfmixing p-Ge laser modes (homodyne mixing) on a GaAs Schottky-barrier diode. The mode structure is determined by the resonator configuration. The crystal length $L = 50$ mm of the Ge sample and the refractive index $n_{Ge} = 3.93$ of Ge determines the axial mode spacing of $\Delta f = 760$ MHz. The mode full width at half mean

(FWHM) of 2.5 MHz is pulse time limited due to the 2 μ s long laser pulse. The line width [6] can be less than 1 MHz for a laser emission pulse length longer than 4 μ s. It is possible to tune the emission in a single line by using an additional tunable external resonator (figure 4(c)). The laser emits with a high output power of several Watts [4]. Unfortunately, such lasers are pulsed and in the past have operated with a low duty cycle [4] of 10^{-5} . Recently, we increased the repetition rate of a low doped Ge:Ga laser up to 250 Hz and improved the duty cycle by one order of magnitude [7] to 1.3×10^{-4} .

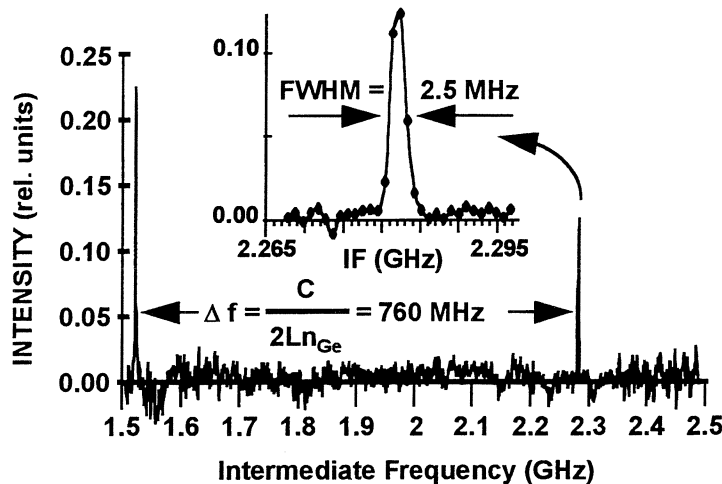


Figure 3. p-Ge single laser pulse emission measured by homodyne mixing on a Schottky diode and with an acousto-optical spectrometer (AOS). The mixing products at the resulting intermediate frequencies (IF) are displayed over a band of 1 GHz with a resolution of 1 MHz determined by the AOS.

4. Crystal preparation and experimental setup

We have studied several Czochralsky-grown Al-doped Ge crystals cut from the same ingot (Table I). The crystals were characterized by variable temperature Hall-effect measurements from 300 K to 6 K. The freeze-out-curve of the free holes gives the majority acceptor and minority donor concentrations [8]. The compensation level for all crystals was less than 1%. The laser crystals were cut into parallelepipeds. Opposing surfaces were parallel within 30 arcsec. Ohmic contacts were formed by implantation of boron with a dose of $2 \times 10^{14} \text{ cm}^{-2}$ at 25 keV and $1 \times 10^{14} \text{ cm}^{-2}$ at 50 keV on two opposite surfaces. The contacts

	N_A (10^{14} cm^{-3})	L (mm)	D (mm)	W (mm)	CO
L1	1.5	30.0	5.0	4.0	[110]
L2	1.2	2.8	3.2	2.8	[100]
L3	1.2	3.3	3.4	3.3	[100]

Table I. Properties of Ge:Al crystals: doping concentration N_A , length L and corresponding crystal orientation CO (lasing direction), distance D between electrical contacts and width W .

were completed by sputtering 20 nm of Pd followed by 200 nm of Au on each side and by annealing at 330 °C for one hour in a N₂ atmosphere.

The high refractive index of Ge enabled laser operation with internal reflection modes (figure 4(a)). We measured the intervalence band emission in the Faraday configuration [9] by immersing the crystals into LHe at 4.2 K and applying electric and magnetic fields. The pulsed electric field was varied in pulse duration and repetition rate. The DC magnetic field was applied with a superconducting coil, e.g., a small thin wire coil of 8 cm length, 3 cm outer diameter and an inner bore of 1 cm with a maximum available magnetic field of 3 T, in which the crystals were mounted. The laser signal was detected with a fast, highly compensated Ge:Ga photodetector and observed directly on a 500 MHz digital oscilloscope.

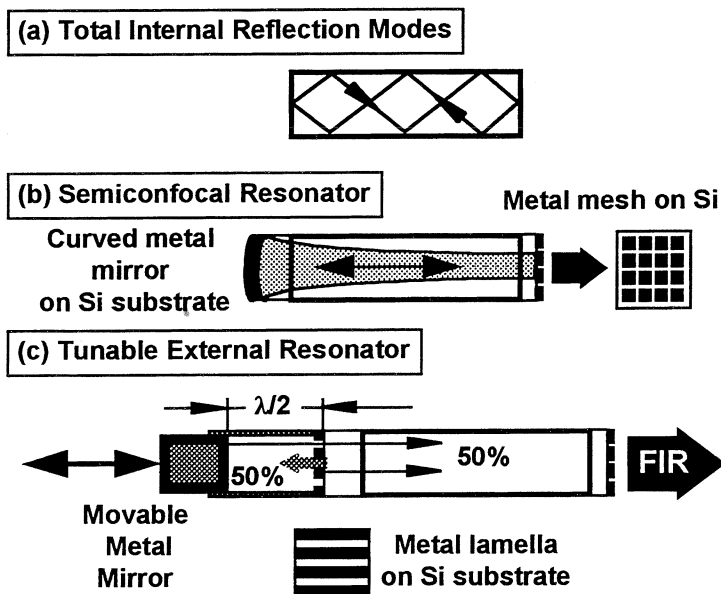


Figure 4. (a) Ge crystal resonator with polished surfaces for total internal reflection modes. (b) External resonator for gaussian beam shape inside the p-Ge crystal. (c) Tunable external resonator for frequency tuning. The lamella structure reflects 50% of the radiation into the crystal while 50% passes through and reflects on the movable back mirror. The frequency is determined by the gap distance while for constructive interference one half of the wavelength has to fit into the cavity.

5. Results

Figure 5(a) shows the lasing regions of the crystals L1 and L2 as a function of the electric field E and magnetic field B . With a reduction of the crystal size, the laser path length inside the crystal decreases, and more frequent internal reflections on lossy surfaces occur. Therefore the size of the lasing regions in the (E, B) plane, the laser pulse length and the laser intensity (figure 5(b)) are decreased.

By connecting a heat sink to one Ohmic contact of L2 we conserved and improved the duty cycle to 1.5×10^{-4} . The power consumption during the electric pulse is reduced from 20 to 2 kW by decreasing the

active volume of L1 to a size of L2 by one order of magnitude [10] to 0.025 cm^3 , e.g., L2 can be operated with a current of 8 A and a voltage as low as 220 V.

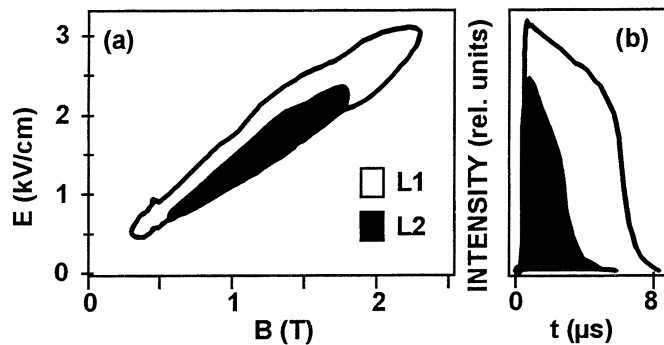


Figure 5. (a) Lasing regions of L1 and L2 with different sizes and doping concentration. (b) Laser pulse intensity measured with a fast Ge:Ga detector.

L3 was specially mounted on a large copper heat sink to enable efficient cooling. Due to the fast heat dissipation we achieved a repetition rate in the order of kHz and a maximum duty cycle of 2×10^{-3} . Figure 6(a) shows magnetic field sweeps for an electric excitation of $4 \mu\text{s}$ length. For a repetition rate of more than 650 Hz the sample cannot cool down to a temperature which enables laser action. The lasing regions shrink to the maximum gain regions with increased temperature and losses.

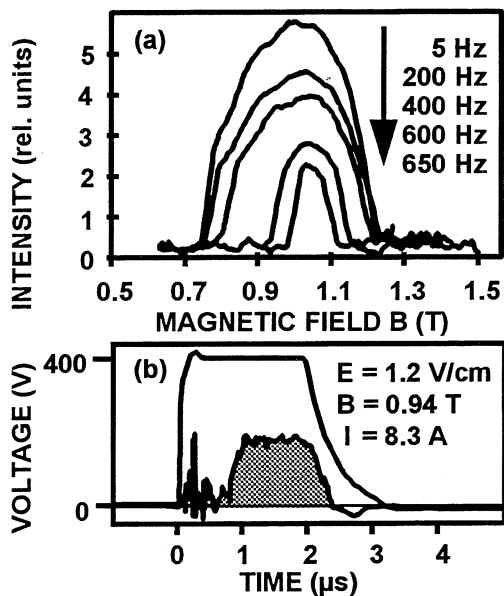


Figure 6. (a) Magnetic field sweeps of L3 at increasing repetition rates for a constant electric field with an electric excitation of $4 \mu\text{s}$. A maximum duty cycle of 0.002 was achieved. (b) Laser pulse (in gray) at a repetition rate of 1000 Hz for a applied voltage of 400 V. Current I, electric field E and magnetic field B are shown. Approximately 7-8 Watts electrical power is dissipated into the liquid helium.

6. Conclusion

The reduced size of our laser crystals leads to lower demands on power supplies, on the size of the magnets and makes small top-table cryostats viable for laser operation. Permanent magnets can be compact (e.g., $(20 \text{ mm})^3$) and can reach magnetic fields up to 1 Tesla. Under high repetition rates the

mean laser crystal temperature reaches temperatures of 15 K which makes it possible in principle to use mechanical cryo-coolers for operating the laser without liquid helium.

Further improvement of the laser geometry, the doping level, the cooling environment, the use of external resonators with mesh outcouplers and uniaxial stress reduces the total applied power and improves the heat dissipation. A 500 μm long p-Ge laser cube would emit mW local oscillator power to pump Schottky diodes in the THz range. Although, the proposed hot electron bolometers would reduce the required power by two to three orders [11,12]. The achieved small size is mainly the result of careful crystal and surface preparation including crystal growth, contact formation and materials characterization.

Acknowledgment - We would like to thank B. Nippe and his colleagues, Institute of Crystal Growth in Berlin, for the optical polishing of the small crystals L2 and L3. We acknowledge the use of facilities at the LBNL operated under US DOE contract DE-AC03-76SF00098.

References

- [1] H.P. Röser, *Infrared Phys.* **32**, 385 (1991).
- [2] R. Titz, M. Birk, D. Hausmann, R. Nitsche, F. Schreier, J. Urban, H. Küllmann, and H.P. Röser, *Infrared Phys. Technol.* **36**, 883 (1995).
- [3] W. Heiss, K. Unterrainer, E. Gornik, W.L. Hansen, and E.E. Haller, *Semicond. Sci. Technol.* **9**, B638 (1994).
- [4] Comprehensive review: E.Gornik, A.A.Andronov (Eds), *Optical & Quant.elec., Special issue* **23**, S111 (1991)
- [5] E.Bründermann and H.P.Röser, *Proc. of the 6th Int. Symposium on Space Terahertz Technology*, 153 (1995)
- [6] E.Bründermann, H.P.Röser, A.V.Muravjov, S.G. Pavlov, and V.N.Shastin, *Infrared Phys. Technol.***1**, 59 (1995)
- [7] E.Bründermann, H.P.Röser, W.Heiss, E.Gornik, and E.E. Haller, *Appl. Phys. Lett.* **67**, 3543 (1995)

- [8] G.E. Stillman and C.M. Wolfe, *Thin Solid Films* **31**, 69 (1976).
- [9] S. Komiyama, S. Kuroda, and T. Yamamoto, *J. Appl. Phys.* **62**, 3552 (1987).
- [10] E. Bründermann, A.M. Linhart, H.P. Röser, O.D. Dubon, W.L. Hansen and E.E. Haller, submitted to *Appl. Phys. Lett.*, accepted for publication (1996).
- [11] A.D. Semenov, R.S. Nebosis, Yu.P. Gousev, M.A. Heusinger and K.F. Renk, *Phys. Rev.* **B52**, 581 (1995)
- [12] D.E. Prober, *Appl. Phys. Lett.* **62**, 2119 (1993)